

Space Structures on the Back of an Envelope: John Hedgepeth's Design Approach

Mark S. Lake*

Composite Technology Development, Inc., Lafayette, Colorado 80026

and

Lee D. Peterson[†] and Martin M. Mikulas[‡]

University of Colorado, Boulder, Colorado 80301

DOI: 10.2514/1.21076

John M. Hedgepeth was among an elite group of engineers who were the main architects of NASA's revolutionary research on large space structures during the 1970s and 1980s. He had an incisive ability to distill, for unique and complex structural design problems, a concise set of primary requirements and compact analytical expressions that relate key design parameters to critical performance metrics. Dr. Hedgepeth and his colleagues derived many such "back-of-the-envelope" expressions to facilitate the design of a wide variety of large space structures. Today, as a new generation of large space structures is being considered, it is timely to revisit Dr. Hedgepeth's approach to the design of these structures. With this motivation, the present paper includes derivations of several back-of-the-envelope solutions, some by the authors and one by Dr. Hedgepeth, to fundamental issues that must be addressed in the design of large space structures. Several conclusions are distilled from these analyses that have broad implication for space structure design.

Nomenclature

\bar{A}	= surface area of reflector
\bar{A}	= average cross-sectional area of members
A_{boom}	= cross-sectional area of truss boom
\mathbf{A}_I	= inertial acceleration vector
A_{longeron}	= cross-sectional area of longeron
A_m	= surface area associated with m th node
a_n	= n th mode participation factor, acceleration
a_{RES}	= accelerometer resolution
a_{rms}	= rms magnitude of acceleration vector
C_{ijkl}	= global stiffness tensor
C_l	= reaction wheel harmonic imbalance
$(C_{1111})_n$	= equivalent axial stiffness of n th group of parallel truss members
c	= imperfection knockdown factor
D	= diameter of reflector
D_{plate}	= equivalent bending stiffness of truss-supported segmented reflector
E	= Young's modulus
$(EA)_n$	= axial stiffness of n th truss member
e_n	= unit length error in n th truss member
\mathbf{F}_I	= d'Alembert inertial force vector
f_c	= isolator corner frequency
f_{ij}	= frequency of mirror vibration mode with greatest effect on the wave front in Hz
f_0	= lowest frequency in Hz
h	= depth of reflector structure
I	= cross-sectional moment of inertia

J_1	= anisotropic bulk modulus (i.e., first invariant of the stiffness tensor)
$[K]$	= stiffness matrix
k	= reflectivity
L	= characteristic spacecraft dimension
\bar{l}	= length of column or truss member
\bar{l}	= average length of truss members
l_n	= length of n th truss member
M	= total number of members in a truss
$[M]$	= mass matrix
M_{column}	= mass of column
M_{sc}	= mass of spacecraft
\hat{N}	= total number of surface nodes in a truss
\hat{N}	= ordered set of unit normal vectors, \hat{n}_m , $m = 1, 2, \dots, M$, from surface nodes
N_{panels}	= number of reflector panels in truss-supported segmented reflector
N_{rings}	= number of rings of reflector panels in truss-supported segmented reflector
N_{struts}	= number of truss struts in truss-supported segmented reflector
n	= number of longerons in a truss boom
\hat{n}_m	= unit normal vector of m th truss node
P	= column compressive load
P_e	= Euler buckling load of column
P_l	= local buckling load of column
P_n	= load in n th truss member
p_s	= solar photon pressure
Q	= strain energy due to member length errors
r	= cross-sectional radius of boom/column
$S_n()$	= function defining unit length error in n th truss member
T_{roll}	= roll period
T_{settle}	= roll settling time
t	= wall thickness of tubular column
t_m	= minimum wall thickness of tubular column
\mathbf{U}	= ordered set of nodal displacement vectors, \mathbf{u}_m , $m = 1, 2, \dots, M$, from member length errors
\mathbf{u}_m	= displacement vector of m th truss node
\bar{w}^2	= mean square displacement of surface nodes
\mathbf{X}_I	= displacement response vector
\mathbf{X}_n	= n th eigenvector (i.e., normal mode)

Presented as Paper 1448 at the the 44th AIAA/ASME/ASCE/AHS/ASC SDM Conference, Norfolk, VA, 7–10 April 2003; received 11 November 2005; revision received 26 April 2006; accepted for publication 27 April 2006. Copyright © 2006 by Mark S. Lake. Published by the American Institute of Aeronautics and Astronautics, Inc., with permission. Copies of this paper may be made for personal or internal use, on condition that the copier pay the \$10.00 per-copy fee to the Copyright Clearance Center, Inc., 222 Rosewood Drive, Danvers, MA 01923; include the code \$10.00 in correspondence with the CCC.

*Chief Engineer, 2600 Campus Drive, Suite D, Associate Fellow AIAA.

[†]Associate Professor, Department of Aerospace Engineering Sciences, Campus Box 429, Associate Fellow AIAA.

[‡]Professor Emeritus, Department of Aerospace Engineering Sciences, Campus Box 429, Fellow AIAA.

x_n	=	n th mode participation factor (displacement)
x_{rms}	=	rms magnitude of displacement vector
δ	=	deformation tolerance
δ_{ij}	=	identity matrix
ε_{ij}	=	global strain tensor
η	=	mass fraction of reflector structure
$(\phi_i)_n$	=	direction cosine between i th coordinate axis and n th group of parallel truss members
λ_{ij}	=	modal eigenvalue
v_n	=	volume fraction of n th group of parallel truss members
ρ	=	material density
ρ_{eq}	=	average volumetric density of uniform truss
ρ_{areal}	=	average areal density of reflector system
σ_e	=	standard deviation of member length errors
$(\sigma_e)_n$	=	standard deviation of length error in n th member
σ_{ij}	=	global stress tensor
σ_l	=	local buckling stress
θ	=	roll angle
v_n	=	n th mode participation factor for displacement due to member length errors
ω_n	=	n th eigenvalue (i.e., normal frequency)
ω_0	=	lowest eigenvalue (i.e., lowest frequency)
ζ	=	modal damping ratio

Introduction

THE rational design of all structures must start with a definition of the task or function of the structure... The successful performance of any structure depends largely on the identification of the critical or primary loads and design criteria on which the design is based.”—J. M. Hedgepeth [1]

John M. Hedgepeth (Fig. 1) served as a research engineer at the NACA Langley Memorial Aeronautics Laboratory from 1948 to 1960, where he became very knowledgeable in structural mechanics. He earned a Ph.D. in Applied Mathematics from Harvard University in 1962, and was very fluent in the language of mathematics. As a result, Dr. Hedgepeth developed an incisive ability to distill, for complex structural design problems, a concise set of primary requirements, which are sufficient for developing and evaluating competing design concepts. Furthermore, Dr. Hedgepeth’s mastery of mathematics and applied mechanics allowed him to reduce mathematically complex design problems into concise, back-of-the-

envelope expressions that relate key design parameters to critical performance metrics. These abilities placed Dr. Hedgepeth among an elite group of engineers who were the main architects of NASA’s revolutionary research on large space structures during the 1970s and 1980s. Dr. Hedgepeth and his colleagues used his back-of-the-envelope approach to structural design to develop numerous creative designs for large space structures [1–34].

Every engineer understands the value of back-of-the-envelope calculations. Without such expressions, the process of structural design would be virtually impossible. Indeed, a structural engineer’s library is incomplete without copies of Roark and Young’s *Formulas for Stress and Strain* [35], Blevin’s *Formulas for Natural Frequency and Mode Shape* [36], and Brush and Almroth’s *Buckling of Bars, Plates, and Shells* [37]. These landmark references include closed-form solutions to a wide variety of common structural response problems. These calculations are sufficient for the sizing of structures that are driven by traditional design criteria. However, as Dr. Hedgepeth astutely predicted, most large space structures are “designed to deal with phenomena as primary criteria which have been considered as only secondary in the past.” [1] Therefore, a large-space-structure engineer’s library must include more than just the traditional references on structural design.

Most concepts for large space structures incorporate a truss as the primary structural element. The present paper includes derivations of several back-of-the-envelope solutions, some by the authors and one by Dr. Hedgepeth, to fundamental problems in the design of trusses for large space structures. All of the solutions presented herein apply to truss structures, and some of the solutions apply to other structural forms such as membrane and inflatable structures. Although these derivations do not exist in the traditional literature on truss design, they are based on traditional concepts from mechanics, dynamics, and stability theory. Similarly, the derivations involve relatively straightforward, although not necessarily obvious, mathematical formulations.

The analyses are focused on several issues that affect substantially the conceptual design of a large space structure. In particular, it is shown that the use of trusses in the construction of large space structures largely derives from consideration of compression-strength efficiency and minimum-gauge construction issues, and that any two truss geometries with the same global stiffnesses must also have the mass (neglecting joint and parasitic masses). Furthermore, it is shown that the magnitudes of deformation of a truss due to either inertial loading or member length error are inversely proportional to the square of its fundamental vibration, which is (in turn) proportional to its depth and the square root of its structural mass. Finally, it is shown that increased damping, either from passive or active means, can reduce the vibration-frequency requirement, and hence the necessary structural depth for a given application.

Effect of Structural Hierarchy on Strength and Mass Efficiency

The advantage of truss structures over other structural forms can be most easily understood by considering two key issues: compression-strength efficiency and minimum-gauge-construction limitations. This section summarizes analyses that compare the mass efficiency of columns loaded in compression [38]. These analyses explore the issues of compression strength and minimum-gauge construction, and consider a variety of structural forms including, but not limited to, trusses (see Fig. 2). A back-of-the-envelope method is developed for comparing the masses of different column concepts, and results show that truss columns are most mass efficient for intermediate-load and lightly loaded applications.

The accepted principle for obtaining the minimum-mass design for a column subjected to compression loading is to design for simultaneous occurrence of the local and global modes of buckling. The column architecture and load class determine the significant buckling modes. Three load classes exist: 1) short columns subjected to high loads, 2) intermediate length columns subjected to intermediate loads, and 3) long columns subjected to light loads. It



Fig. 1 John M. Hedgepeth, Ph.D.

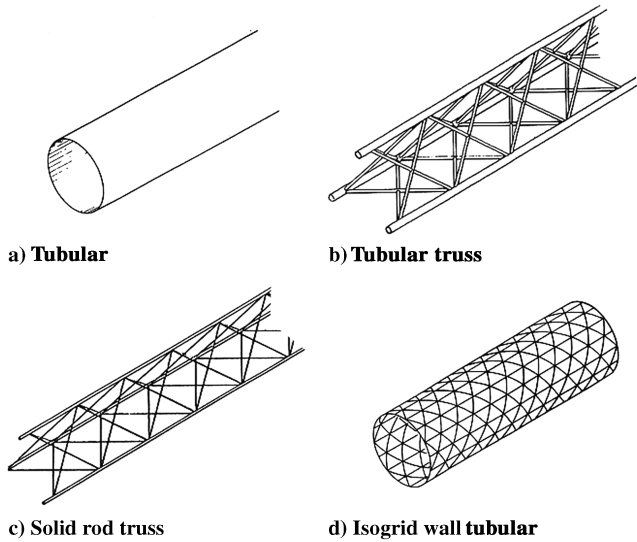


Fig. 2 Column concepts considered.

has been shown that large space structures typically fall within the intermediate-load and lightly loaded categories.

For columns of intermediate load and length, local and global buckling dominate the design. Consider a thin-walled tubular column (Fig. 2a). The Euler buckling load for such a column is

$$P_e = \frac{\pi^2 EI}{l^2} = \frac{\pi^3 E r^3 t}{l^2} \quad (1)$$

where r is the tube radius, t is the tube thickness, l is the column length, and E is Young's modulus of the material. The load at which local wall buckling occurs is [38]

$$P_l = \sigma_l(2\pi r t) = 1.2c\pi E t^2 \quad (2)$$

Finally, the mass of the tubular column is

$$M_{\text{column}} = \rho A l = \rho(2\pi r t l) \quad (3)$$

Equating the buckling loads given by Eqs. (1) and (2) to P gives expressions for the optimum radius and thickness in terms of P , E , c , and l . Substituting these expressions into Eq. (3) gives the following optimum mass expression for a tubular column in the intermediate-load range:

$$M_{\text{column}} = \left(\frac{2}{0.3\pi c} \right)^{\frac{1}{3}} \frac{\rho}{E^{2/3}} P^{\frac{1}{3}} l^{\frac{5}{3}} \quad (4)$$

For long, lightly loaded columns, the wall thickness reaches a practical minimum and for lower loads, local wall buckling does not

occur. For such columns, only Euler buckling is critical and the minimum wall thickness is a constant. The optimum mass equation for such a condition is determined by eliminating r from Eqs. (1) and (3), and is given by

$$M_{\text{column}} = 2t_m^{2/3} \frac{\rho}{E^{1/3}} P^{\frac{1}{3}} l^{\frac{5}{3}} \quad (5)$$

Equations (4) and (5) can be rearranged such that they relate a set of standard structural design parameters [38]. The standard structural design expression for intermediate-load column design is obtained by dividing Eq. (1) by $l^{5/3}$ and grouping the resulting equation as follows:

$$\frac{M_{\text{column}}}{l^{5/3}} = \left(\frac{2}{0.3\pi c} \right)^{\frac{1}{3}} \times \frac{\rho}{E^{2/3}} \times P^{\frac{1}{3}} \quad (6)$$

where $M_{\text{column}}/l^{5/3}$ is the mass parameter, $(2/0.3\pi c)^{1/3}$ is the shape factor, $\rho/E^{2/3}$ is the material parameter, and $P^{1/3}$ is the loading index. Similarly, the standard structural efficiency expression for long, lightly loaded column design is obtained by dividing Eq. (6) by $l^{5/3}$ and grouping as:

$$\frac{M_{\text{column}}}{l^{5/3}} = 2t_m^{2/3} \times \frac{\rho}{E^{1/3}} \times P^{\frac{1}{3}} \quad (7)$$

where $M_{\text{column}}/l^{5/3}$ is the mass parameter, $2t_m^{2/3}$ is the shape factor, $\rho/E^{1/3}$ is the material parameter, and $P^{1/3}$ is the loading index.

Equations (6) and (7) are written in terms of the four parameters critical for the design of a compressively loaded column: a mass parameter, a cross-sectional shape factor, a material parameter, and a loading index. These expressions were derived for the tubular column shown in Fig. 2a. Similar mass equations have been derived for the other column forms presented in Fig. 2, and these equations differ primarily in the cross-sectional shape factor [38]. The mass parameter is the same in all cases, and the material parameters and loading indices vary primarily in their exponents.

Figure 3 presents a logarithmic plot that compares the masses of all of the column concepts shown in Fig. 2. In this figure, the mass parameter, $M_{\text{column}}/l^{5/3}$, is plotted vs the applied compression load P . For all column designs considered, $\log(M_{\text{column}}/l^{5/3})$ varies linearly with $\log(P)$. Hence, this method of "normalizing" the mass, length, and load parameters provides a very convenient basis for comparing the mass efficiency of competing designs. The comparison demonstrates that truss columns are lighter in weight than tubular columns for all but very high loads. Similarly, isogrid columns are most efficient for certain combinations of load and length. In general, columns with a greater degree of hierarchy (i.e., structural detail) result in lighter-weight designs.

Effect of Lattice Geometry on Truss Stiffness and Mass Efficiency

Given that a truss structure is more mass efficient than other structural forms, one might ask further, what is the most efficient truss lattice for a given application? Although the answer to this question might be complicated by practical considerations, such as requirements for interfacing the truss to other spacecraft elements, the answer is rather simple if one considers only specific stiffness (i.e., stiffness-to-mass ratio). Following is a proof that all trusses are equally efficient on the basis of specific stiffness alone [39].

The present derivation applies to any uniform truss, which is any truss generated by rotational and/or translational replication of a characteristic cell as shown in Fig. 4. It is assumed that the repeating cell is small in comparison to the size of the truss, and thus finite boundary effects are not explicitly addressed. It is also assumed that parasitic mass, such as the mass of joints, is negligible or the same for any truss geometry. Finally, it is assumed that the global elastic behavior of the truss can be modeled by an equivalent anisotropic continuum [40]. The elastic constants, C_{ijkl} , that characterize the truss appear in the following tensor form of the constitutive equation:

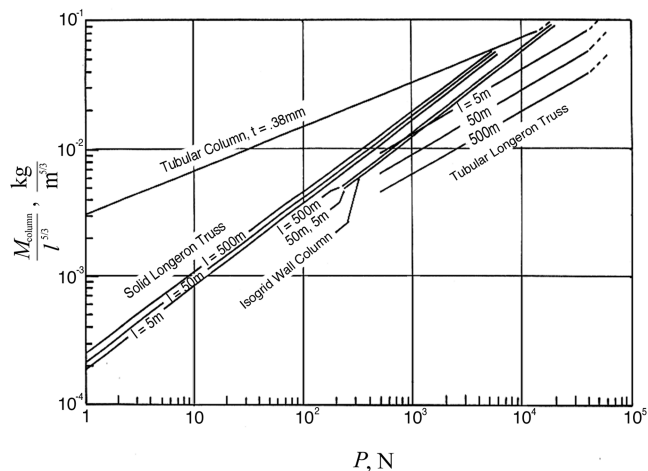


Fig. 3 Comparison of column masses.

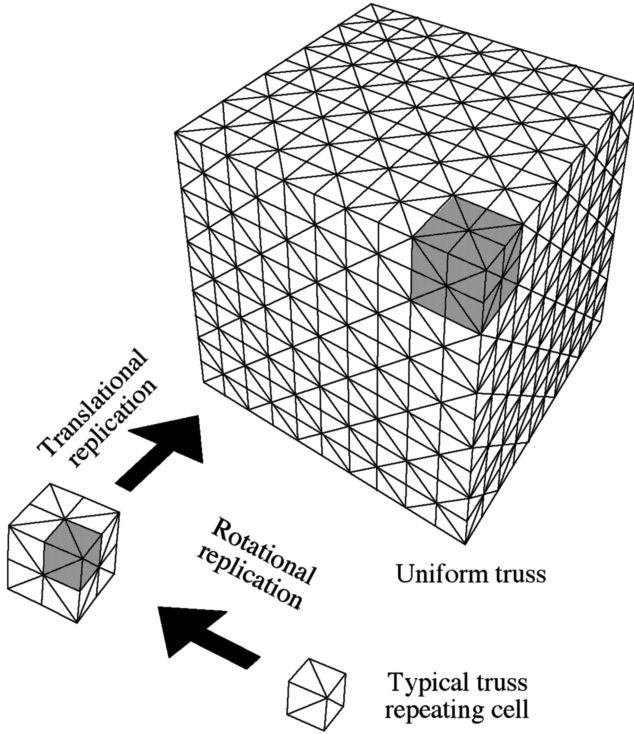


Fig. 4 Uniform truss generated from repeating cell.

$$\sigma_{ij} = C_{ijkl} \varepsilon_{kl} \quad (8)$$

The equivalent continuum theory for uniform trusses is mathematically similar to laminated plate theory. The members within the truss lattice are divided into groups of parallel members. Since truss members carry only axial load, each group of parallel members can be modeled as a unidirectional elastic continuum that has no transverse or shearing stiffnesses. The equivalent axial stiffness of each group of parallel members is determined using the rule of mixtures. The generalized stiffnesses for the truss assemblage are obtained by superimposing the stiffnesses of each of the groups of parallel members.

The equivalent axial stiffness for the n th group of parallel members is

$$(C'_{1111})_n = E v_n \quad (9)$$

where E is the Young's modulus of the material in the members and v_n is the volume fraction of the group of members (i.e., the ratio of the total volume of material in the members to the total volume of the truss).

The generalized anisotropic stiffnesses for the truss are calculated by transforming the unidirectional stiffnesses for each of its groups of

parallel members into a global coordinate system, and summing the results as indicated by

$$C_{ijkl} = \sum_n (C'_{1111})_n (\phi_i \phi_j \phi_k \phi_l)_n = \sum_n E v_n (\phi_i \phi_j \phi_k \phi_l)_n \quad (10)$$

where $(\phi_i)_n$ is the direction cosine between the longitudinal axis of the truss members in the n th group and the i th global coordinate axis. Assuming E is the same for all truss members, Eq. (10) becomes

$$C_{ijkl} = E \sum_n v_n (\phi_i \phi_j \phi_k \phi_l)_n \quad (11)$$

The first of three invariant quantities for the anisotropic stiffness tensor is called the anisotropic bulk modulus and is defined as [41]

$$J_1 \equiv C_{1111} + C_{2222} + C_{3333} + 2C_{2233} + 2C_{1133} + 2C_{1122} \quad (12)$$

Substituting Eq. (11) into Eq. (12) gives

$$J_1 = E \sum_n v_n (\phi_1^2 + \phi_2^2 + \phi_3^2)_n^2 = E \sum_n v_n \quad (13)$$

Note the sum of the squares of the three direction cosines must be equal to unity regardless of the orientation of the group of parallel members. Therefore, Eq. (13) simplifies to the very compact result that the anisotropic bulk modulus is equal to the modulus of the members times the sum of their volume fractions.

The equivalent continuum density of the truss lattice is defined as the total mass of material within the lattice divided by the volume of space occupied by the truss. Thus, the equivalent density is defined by

$$\rho_{eq} \equiv \rho \sum_n v_n \quad (14)$$

Dividing Eq. (13) by Eq. (14) gives

$$\frac{J_1}{\rho_{eq}} = \frac{E}{\rho} \quad (15)$$

Equation (15) is a surprisingly compact result that ensures the continuum anisotropic bulk modulus-to-density ratio of any uniform truss structure is equal to the specific modulus (i.e., E/ρ) of the material in the truss members. In other words, all truss lattices constructed of the same material (or materials with the same specific modulus) must have the same bulk modulus-to-density ratio. Equation (15) guarantees that any two trusses that are made from the same material, have the same continuum stiffnesses, and occupy the same volume *must also have the mass*. This result essentially guarantees that there is no optimum truss on the basis of stiffness efficiency. Thus, a designer is at liberty to select the truss geometry based on other design requirements without risk of sacrificing stiffness efficiency.

Consider a more specific example of the design of a truss boom, such as the three- and four-longeron truss booms sketched in Fig. 5. The equivalent bending stiffnesses of a truss boom with n longerons equally spaced at a radius of r from the center of the cross section is [38]

$$EI = \frac{nEA_{longeron}r^2}{2} = \frac{EA_{boom}r^2}{2} \quad (16)$$

where $A_{longeron}$ is the cross-sectional area of each longeron, A_{boom} is the sum of the cross-sectional areas of all of the longerons, and $A_{longeron} = A_{boom}/n$. Equation (16) indicates that any two truss booms with the same diameter and bending stiffness must incorporate the same amount of material in their longerons, regardless of the number of longerons. Assuming that the mass of the battens, diagonals, and joint fittings (i.e., parasitic mass) are the same regardless of the number of longerons, this result implies that different truss booms with equal bending stiffness, cross-sectional diameter, and incorporating the same longeron material, must weigh the same.

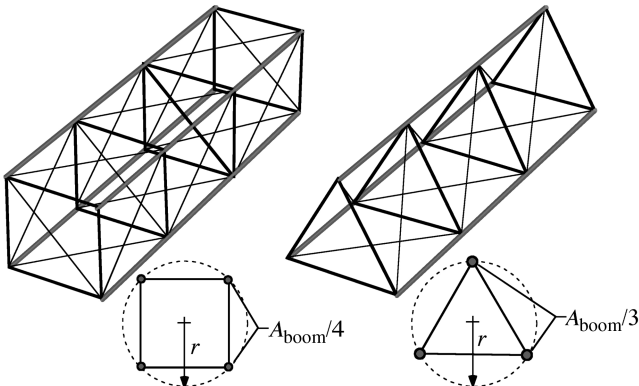


Fig. 5 Three- and four-longeron truss booms.

Effect of Structural Depth and Mass Fraction on Vibration Frequency

Most large-space-structures are designed to support science or communication instruments, such as radio-frequency antennas or optical telescopes. These structures must be dimensionally stable and are usually designed to meet a vibration-frequency requirement. This section is intended to convey some insight into the problem of designing a large-space-structure to meet a vibration-frequency requirement. A truss-supported segmented reflector is considered in these analyses (see Fig. 6), but similar results have been determined for other structural configurations [42]. An explicit analytical expression is derived for the fundamental frequency of the reflector. This expression is written in terms of three key design parameters: structural mass fraction, structural depth-to-diameter ratio, and material specific stiffness. This expression is used to illustrate the trade that can be made between mass fraction and depth to meet a vibration-frequency requirement.

In [43] it is shown that, for large diameter-to-depth ratios, the fundamental free-free frequency of a truss-supported segmented reflector can be approximated by the frequency of an equivalent flat, circular, sandwich-plate as shown in the left sketch in Fig. 6. In these analyses the reflector panels, mechanical joints, and any other nonstructural components are treated as parasitic mass and the stiffness is determined from the truss only. The general solution for the fundamental, free-free vibration frequency f_0 (in Hz) is then

$$f_0 = \frac{3.343}{D^2} \sqrt{\frac{D_{\text{plate}}}{\rho_{\text{areal}}}} \quad (17)$$

where the equivalent plate bending stiffness and areal density are given, respectively, by

$$D_{\text{plate}} = \sqrt{3} E \bar{A} \bar{I} / 4 \quad \rho_{\text{areal}} = \frac{1}{\eta} \left[\frac{N_{\text{struts}} \rho \bar{A} \bar{I}}{3 \sqrt{3} D^2 / 8} \right] \quad (18)$$

where $E \bar{A} \bar{I}$ and $\rho \bar{A} \bar{I}$ are the average axial stiffness and mass of each strut in the support truss, N_{struts} is the number of members in the support truss, and η is the structural mass fraction of the support truss defined as

$$\eta \equiv \frac{\text{truss mass}}{\text{total mass}} \quad (19)$$

Substituting Eqs. (18) into Eq. (17) and simplifying gives

$$f_0 = \frac{1.773}{D} \sqrt{\frac{\eta}{N_{\text{struts}}}} (E/\rho) \quad (20)$$

Figure 7 presents sketches of three truss-supported segmented reflectors with two to four rings of reflector panels, respectively. Also included are the number of reflector panels and truss struts each and

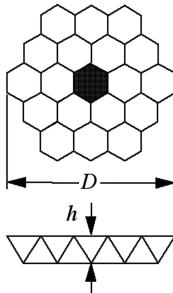
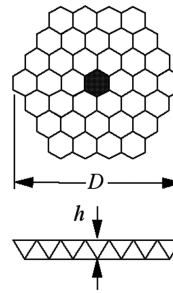
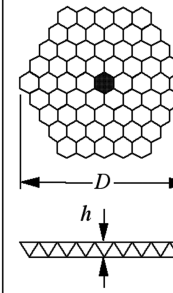
$N_{\text{rings}} = n$ $N_{\text{panels}} = 3n(n+1)$ $N_{\text{struts}} \approx 13(2n+1)^2/2$ $D/h \approx (2n+1)\sqrt{3}/2$		
$N_{\text{rings}} = 2$ $N_{\text{panels}} = 18$ $N_{\text{struts}} = 156$ $D/h = 5\sqrt{3}/2$	$N_{\text{rings}} = 3$ $N_{\text{panels}} = 36$ $N_{\text{struts}} = 315$ $D/h = 7\sqrt{3}/2$	$N_{\text{rings}} = 4$ $N_{\text{panels}} = 60$ $N_{\text{struts}} = 528$ $D/h = 9\sqrt{3}/2$
		

Fig. 7 Part counts and diameter-to-depth ratios for truss-supported segmented reflectors.

general expressions for these part counts as functions of the number of rings of panels, N_{rings} . Finally, Fig. 7 includes a general expression for the truss depth ratio D/h as a function of N_{rings} . From these expressions, it can be shown that

$$N_{\text{struts}} \approx \frac{13}{3} (D/h)^2 \quad (21)$$

Substituting Eqs. (21) into Eq. (20) gives

$$f_0 = \frac{0.852}{D} (h/D) \sqrt{\eta(E/\rho)} \quad (22)$$

Equation (22) is an approximate expression for the fundamental free-free vibration frequency (in Hz) of a truss-supported segmented reflector. The frequency is proportional to the depth-to-diameter ratio h/D , and the square root of the structural mass fraction η , and the specific modulus, E/ρ of the truss. Also, the frequency is inversely proportional to the diameter D . Analyses of other mirror structural architectures show similar vibration-frequency relationships [42]. Therefore, for a given diameter reflector, the key structural design parameters that affect the vibration frequency are structural mass fraction and depth-to-diameter ratio. In general, proper design of large space structures to satisfy a vibration-frequency requirement requires a trade between structural depth and structural mass. Specifically, for a given frequency requirement, an increase in structural depth allows a decrease in structural mass, and vice versa.

Effect of Vibration Frequency on Truss Deformation Under Inertial Loading

The inertial loads that can affect the dimensional precision of a large-space-structure include slow loads, gravity gradient loads, and solar- and atmospheric-drag loads. In general, these inertial loads are slowly varying in time, and structural distortions due to these loads can be estimated by static-response analysis. This section presents a derivation of an upper bound on the rms deformation in a large-space-structure due to static inertial loads [42]. The result of this derivation indicates that deformations due to inertial loading are inversely proportional to the square of the fundamental vibration frequency of the structure, regardless of the size and shape of the structure.

Consider that a large-space-structure can be represented as an n -DOF elastic system characterized by a mass matrix and stiffness matrix. For this system, there exists an orthonormal set of eigenvectors X_n that satisfy

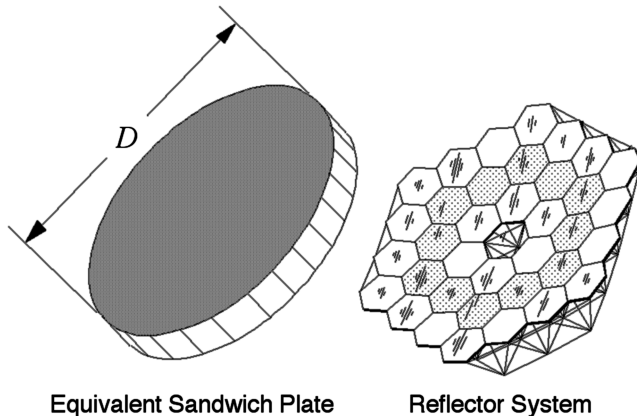


Fig. 6 Equivalent sandwich-plate model of truss-supported segmented reflector.

$$\frac{1}{\omega_n^2} \mathbf{X}_n = [\mathbf{K}]^{-1} [\mathbf{M}] \mathbf{X}_n \quad (23a)$$

$$(\mathbf{X}_m)^T \mathbf{X}_n = \delta_{mn} \quad (23b)$$

where ω_n are the eigenvalues (i.e., natural frequencies) associated with the eigenvectors, \mathbf{X}_n .

Consider an inertial loading of the system defined by the following vector of d'Alembert forces \mathbf{F}_I :

$$\mathbf{F}_I = [\mathbf{M}] \mathbf{A}_I \quad (24)$$

Following the principle of d'Alembert, the deformations \mathbf{X}_I resulting from this load can be determined from the following equivalent static problem:

$$\mathbf{X}_I = [\mathbf{K}]^{-1} [\mathbf{M}] \mathbf{A}_I \quad (25)$$

Without loss of generality, the inertial acceleration vector and the inertial deformation vector can be expressed in terms of the basis of normal modes \mathbf{X}_n as follows:

$$\mathbf{X}_I = x_n \mathbf{X}_n \quad (26a)$$

$$\mathbf{A}_I = a_n \mathbf{X}_n \quad (26b)$$

where, by definition

$$x_n \equiv (\mathbf{X}_n)^T \mathbf{X}_I \quad (27a)$$

$$a_n \equiv (\mathbf{X}_n)^T \mathbf{A}_I \quad (27b)$$

Substituting Eqs. (26) into Eq. (25) gives

$$x_n \mathbf{X}_n = a_n [\mathbf{K}]^{-1} [\mathbf{M}] \mathbf{X}_n \quad (28)$$

Substituting the identity from Eq. (23a) into Eq. (28) gives

$$x_n \mathbf{X}_n = \frac{a_n}{\omega_n^2} \mathbf{X}_n$$

which, for any nonzero mode \mathbf{X}_n , reduces to the following identity:

$$x_n = \frac{a_n}{\omega_n^2} \quad (29)$$

The general solution for the deformation due to inertial loading is found by substituting Eq. (29) into Eq. (26a):

$$\mathbf{X}_I = \frac{a_n}{\omega_n^2} \mathbf{X}_n \quad (30)$$

The rms magnitude of deformation is given by the norm (i.e., the square root of the inner product) of the deformation vector. Recalling that the basis of normal modes satisfy Eq. (23b), the rms magnitude of deformation reduces to

$$x_{\text{rms}} = \sqrt{(\mathbf{X}_I)^T \mathbf{X}_I} = \sqrt{\sum_n \left(\frac{a_n}{\omega_n^2} \right)^2} \quad (31)$$

Similarly, from Eq. (26b) the rms magnitude of the inertial acceleration a_{rms} reduces to

$$a_{\text{rms}} = \sqrt{\sum_n a_n^2} \quad (32)$$

Note that Eqs. (31) and (32) are exact if all modes (i.e., all values of n) are included in the summation.

Equation (31) can be modified by normalizing the vibration frequencies ω_n by the lowest (i.e., fundamental) vibration frequency ω_0 . The result is

$$x_{\text{rms}} = \frac{1}{\omega_0^2} \sqrt{\sum_n a_n^2 \left(\frac{\omega_0}{\omega_n} \right)^4} \quad (33)$$

Because $(\omega_0/\omega_n) \leq 1$, Eqs. (32) and (33) lead to the following upper bound for the deformation magnitude:

$$x_{\text{rms}} \leq \frac{a_{\text{rms}}}{\omega_0^2} \leq \frac{a_{\text{rms}}}{4\pi^2 f_0^2} \quad (34)$$

where f_0 is the vibration frequency (in Hz) of the fundamental mode and a_{rms} is the rms magnitude of the acceleration associated with the disturbance load.

A very significant result of Eq. (34) is that it does not include any structural dimensions. Hence, two different sized (and shaped) structures with equal vibration frequencies can be expected to have similar deformation magnitudes in response to the same inertial loading.

Effect of Member Length Errors on Truss Surface Accuracy

This section presents analyses derived by John Hedgepeth to study the relationship between member length errors and the resulting global dimensional errors in large truss-supported reflector structures [18]. Similar to the previous analyses of inertial-load deformations, these analyses are based on a modal expansion of the displacement field within the truss. The analyses are general and apply to any three-dimensional lattice structure, however, the intent is to examine precision reflector structures like that shown in Fig. 8. Note, the present derivation adopts a slightly different nomenclature than that used in [18] to avoid confusion with other nomenclature presented herein.

Consider that the surface of the reflector truss contains a total of M nodes and that associated with any m th node is a surface area A_m and a unit normal vector $\hat{\mathbf{n}}_m$ (see Fig. 8). Let \mathbf{u}_m be the displacement vector of the m th node from the theoretically perfect location of the node. Then, the weighted mean square of the normal surface distortion is

$$\bar{w}^2 = \frac{1}{A} \sum_{m=1}^M A_m (\hat{\mathbf{n}}_m \cdot \mathbf{u}_m)^2 \quad (35)$$

where A is the total surface area of the reflector truss given by

$$A = \sum_{m=1}^M A_m \quad (36)$$

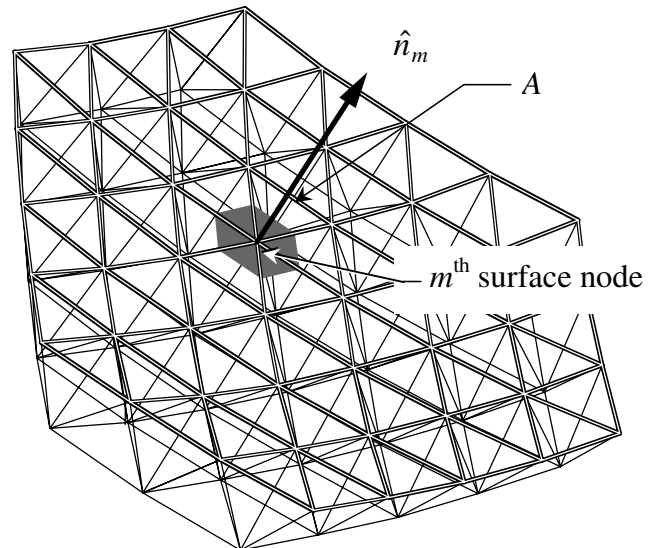


Fig. 8 Typical reflector truss.

In this analysis, the nodal displacements \mathbf{u}_m , arise from errors in the lengths of the truss members. Because the distortion of the surface is the desired result, it is assumed that the displacement degrees of freedom associated with the surface nodes are adequate to describe the elastic response of the entire truss. The set of displacement variables $\{\mathbf{U}\}$ is then defined as the ordered set of displacements, \mathbf{u}_m , as shown in Eq. (37a). Similarly, an ordered set of the surface normal vectors $\{\hat{\mathbf{N}}\}$ and an equivalent mass matrix $[\mathbf{M}]$ can be defined as in Eqs. (37b) and (37c).

$$\{\mathbf{U}\} = \begin{Bmatrix} \mathbf{u}_1 \\ \vdots \\ \mathbf{u}_M \end{Bmatrix} \quad (37a)$$

$$\{\hat{\mathbf{N}}\} = \begin{Bmatrix} \hat{\mathbf{n}}_1 \\ \vdots \\ \hat{\mathbf{n}}_M \end{Bmatrix} \quad (37b)$$

$$[\mathbf{M}] = \rho_{\text{areal}} \begin{bmatrix} A_1 & 0 & 0 \\ 0 & \ddots & 0 \\ 0 & 0 & A_M \end{bmatrix} \quad (37c)$$

where ρ_{areal} is the average areal density of the reflector structure.

Substituting Eqs. (37a–37c) into Eq. (35) gives the following for the weighted mean square of the normal surface distortion:

$$\bar{w}^2 = \frac{1}{\rho_{\text{areal}} A} \{\mathbf{U}\}^T ([\mathbf{M}]\{\hat{\mathbf{N}}\}\{\hat{\mathbf{N}}\}^T)\{\mathbf{U}\} \quad (38)$$

where the matrix $[\mathbf{M}]\{\hat{\mathbf{N}}\}\{\hat{\mathbf{N}}\}^T$ is a mass matrix that has been weighted by the vector of surface normal displacements. This weighted mass matrix nulls out the contribution of displacement components within the plane of the reflector surface by assigning the effective mass for these degrees of freedom to be zero.

Consider now the cause of the surface distortion: the errors in the lengths of the truss members. Let the total number of members in the truss be N and the unit length error in the n th member be e_n . The load in the n th member can be expressed as:

$$P_n = (EA)_n [S_n(\{\mathbf{U}\}) - e_n] \quad (39)$$

where $S_n(\{\mathbf{U}\})$ is a function defining the unit length error between the endpoints of the n th member due to the displacements of the surface nodes in the truss, and $(EA)_n$ is the extensional stiffness of the member. The function S_n is assumed to be linear and homogeneous. The total strain energy due to these member loads is

$$Q = \frac{1}{2} \sum_{n=1}^N (EA)_n l_n \{[S_n(\{\mathbf{U}\})]^2 - 2e_n S_n(\{\mathbf{U}\}) + e_n^2\} \quad (40)$$

where l_n is the length of the n th member.

The nodal displacements $\{\mathbf{U}\}$ can be expanded in terms of a set of orthogonal modes, or eigenvectors $\{\mathbf{X}_m\}$ for the structure

$$\{\mathbf{U}\} = v_m \{\mathbf{X}_m\} \quad (41)$$

where v_m is the modal participation factor for the m th mode. A set of orthogonal eigenvectors can be constructed using Eqs. (23a) and (23b), but this would result in a set of $3M$ eigenvectors for the $3M$ surface node displacement variables. Because only the normal displacements of the surface nodes are of interest here, an orthonormal set of M eigenvectors $\{\mathbf{X}_m\}$ is constructed using the following orthonormality condition:

$$\frac{1}{\rho_{\text{areal}} A} \{\mathbf{X}_i\}^T ([\mathbf{M}]\{\hat{\mathbf{N}}\}\{\hat{\mathbf{N}}\}^T)\{\mathbf{X}_j\} = \delta_{ij} \quad (42)$$

where δ_{ij} is the identity matrix ($\delta_{ij} = 0$ for $i \neq j$, and $\delta_{ij} = 1$ for $i = j$). These eigenvectors must also diagonalize the potential

energy. That is

$$\frac{1}{\rho_{\text{areal}} A} \sum_{n=1}^N (EA)_n l_n S_n(\{\mathbf{X}_i\}) S_n(\{\mathbf{X}_j\}) = \delta_{ij} \omega_i^2 \quad (43)$$

Substituting the expansion, Eq. (41), into Eq. (38) and using Eq. (42) gives

$$\bar{w}^2 = \sum_{m=1}^M v_m^2 \quad (44)$$

Similarly, substituting Eq. (41) into Eq. (40) and using Eq. (43) and minimizing the total potential energy Q , with respect to v_m gives

$$v_i = \frac{1}{\rho_{\text{areal}} A \omega_i^2} \sum_{n=1}^N l_n e_n (EA)_n S_n(\{\mathbf{X}_i\}) \quad (45)$$

Substituting Eq. (45) into Eq. (44) gives

$$\begin{aligned} \bar{w}^2 &= \sum_{i=1}^M \frac{1}{\rho_{\text{areal}}^2 A^2 \omega_i^4} \sum_{k=1}^N \sum_{j=1}^N [l_j e_j (EA)_j S_j(\{\mathbf{X}_i\})] [l_k e_k (EA)_k S_k(\{\mathbf{X}_i\})] \\ &= \sum_{i=1}^M \frac{1}{\rho_{\text{areal}}^2 A^2 \omega_i^4} \sum_{k=1}^N \sum_{j=1}^N [l_j e_j (EA)_j S_j(\{\mathbf{X}_i\})] [l_k e_k (EA)_k S_k(\{\mathbf{X}_i\})] \end{aligned} \quad (46)$$

Here it is assumed that the member length errors e_n are random and, therefore, are statistically independent. Further, it is assumed that the mean error is zero and the standard deviation of all member errors is σ_e . Finally, it is assumed that the standard deviation in error for the n th member, $(\sigma_e)_n$, is scaled relative to the extensional stiffness and length of the member. Defining the mean extensional stiffness and length for all members to be $E\bar{A}$ and \bar{l} , respectively, this relationship between σ_e and $(\sigma_e)_n$ can be written as

$$(\sigma_e)_n = \frac{E\bar{A}\bar{l}}{(EA)_n l_n} \sigma_e \quad (47)$$

Considering the statistical independence of the member length errors, the double summation in Eq. (46) collapses to a single summation. Applying Eq. (43), this single summation further simplifies as follows:

$$\langle \bar{w}^2 \rangle = \frac{E\bar{A}\bar{l}\sigma_e^2}{\rho_{\text{areal}} A} \sum_{i=1}^M \frac{1}{\omega_i^2} \quad (48)$$

where $\langle \bar{w}^2 \rangle$ is the “expectation” of the weighted mean square surface distortion due to the standard deviation σ_e in member length errors.

Thus, the mean square surface distortion is expressed as the sum of the inverse squares of the natural frequencies of the structure. This remarkably simple result is similar to the result presented in Eq. (34) for the distortion of a reflector structure due to inertial loads. In both cases, deformations are shown to be proportional to the inverse square of the natural frequency. In general, it is typically seen that stiffness-driven response (even under static loading) in large-space-structures is proportional to the inverse square of the fundamental vibration frequency.

Effect of Passive and Active Damping on the Required Structural Frequency

Any structural design in which dynamic loading is a concern should consider not only vibration frequency but also damping. For many applications, vibration frequency has a significant effect on the level of damping that is necessary and vice versa [42]. Whether this damping comes from passive devices or active-control systems is a key trade that should be considered in the conceptual design. In general, low levels of damping can be achieved through purely passive design, whereas high levels of damping require active structural control. In this section, a method is proposed for allocating structural frequency and passive-damping requirements and

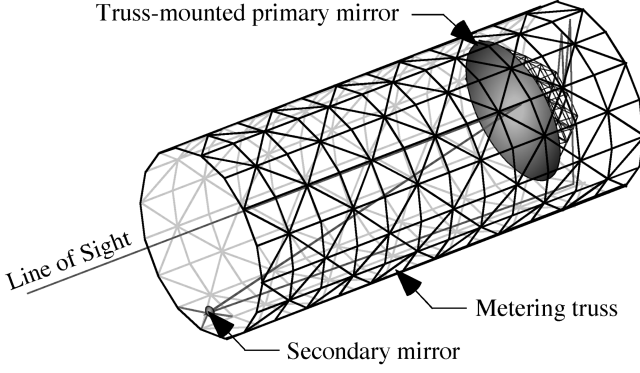


Fig. 9 Large space telescope concept.

balancing these with active-control requirements. The method is based on the construction of functions that relate design constraints to fundamental frequency f_0 and damping ζ . By plotting these constraint functions on an f_0 vs ζ plot, the dominant constraint becomes readily apparent, and the necessary damping is clearly defined.

To illustrate the methodology, a large space telescope is considered. The telescope includes a 4-m-diam, truss-supported, primary mirror, which is connected to a secondary mirror through a 12-m-long metering truss (see Fig. 9). A typical observation would begin by slewing the telescope to point at the target star and maintaining this inertial alignment using reaction wheel actuators (RWA). After this, the thermal environment would be allowed to stabilize at the new orientation. Then a deformable tertiary mirror would be statically adjusted to remove any remaining wave front error. The stability of this optical wave front must be maintained by the primary mirror structure during a subsequent observation. The dimensional stability requirement for the primary mirror structure to maintain this wave front is $\delta = 18$ pm.

Four constraint functions that relate fundamental frequency and damping are defined for this telescope structure. The first three constraint functions are derived from three applied load conditions: 1) roll and settle about the line of sight, 2) resonance of the structure by an imbalance in the RWA, and 3) acceleration due to static solar pressure. The fourth constraint function is derived from considering the resolving power of an accelerometer mounted on the primary mirror structure for the active-control system. These constraint functions are presented next without derivation.

The first constraint function requires structural deformations, which are induced during a slew maneuver, to be damped out in a finite time. This roll and settle load constraint assumes a “bang-bang” torque profile is applied to the spacecraft. When the maneuver is completed, the static deformation due to the roll acceleration becomes the initial condition for the damped free decay vibration that follows. If this free decay is required to be within a required tolerance δ at the end of the settling time, the following (f_0, ζ) constraint must be satisfied:

$$\delta \geq \frac{L\theta}{T_{\text{Roll}}^2} \cdot \frac{1}{\pi^2 f_0^2} e^{-2\pi\zeta f_0 T_{\text{Settle}}} \quad (49)$$

The second constraint function considers dynamic loads produced by an imbalance in the RWA. These disturbances consist of harmonic, subharmonic, and superharmonic components [44]. Ordinarily, a vibration isolator is used to reduce the RWA disturbances. This can be reasonably modeled using a second-order roll-off with a corner frequency as a design parameter. However, even with this isolation, resonance of the structure by the RWA can be a concern. Requiring the resonance of the lowest mode to be within the tolerance δ results in the following (f_0, ζ) constraint:

$$f_0 \geq f_c \sqrt{\frac{C_1}{2\sqrt{2}\pi^2\zeta M_{\text{sc}}\delta}} - 1 \quad (50)$$

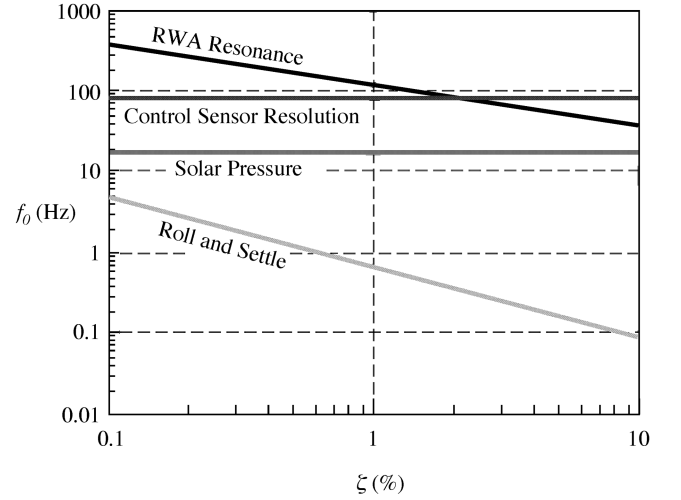


Fig. 10 Primary mirror frequency requirement for $\delta = 18$ pm surface accuracy.

The third constraint function considers the deformation of the mirror due to solar pressure [45]. Although this loading produces a small acceleration, the deformations could be significant for a large space telescope. This loading is static, and so the corresponding (f_0, ζ) constraint does not depend on damping:

$$f_0 \geq \frac{1}{\pi} \sqrt{\frac{p_s A}{2M_{\text{sc}}\delta}} \quad (51)$$

The final constraint function considers the practical implications of sensing structural vibration for active structural damping and control. The acceleration produced by a structural vibration depends upon the frequency of that vibration. For the vibration to produce a resolvable level of acceleration, the lowest mode of the structure is further constrained by

$$f_0 \geq \frac{1}{2\pi} \sqrt{\frac{a_{\text{RES}}}{\delta}} \quad (52)$$

where a_{RES} is the measurement resolution of an accelerometer mounted on the structure.

Figure 10 plots the (f_0, ζ) constraint functions defined by Eqs. (49–52). A dimensional stability requirement $\delta = 18$ pm is assumed and values for other performance parameters are specified in Table 1. The frequency requirement for the primary reflector is the largest of the four constraint values for a given damping level. For example, at a damping ratio of 1% (perhaps typical for passive-damping designs), the driving condition is RWA resonance, which requires a frequency of approximately 100 Hz. Above a damping ratio of approximately 2%, the driving condition is the control sensor (i.e., accelerometer) resolution, which requires a frequency of about 90 Hz. Note that above this damping level, the requirement on the structural frequency remains constant. Hence, one might infer that

Table 1 Large Telescope Performance Parameters

Parameter	Value
θ	45 deg
T_{roll}	600 s
T_{settle}	300 s
L	12 m
f_c	1 Hz
C_1	0.38 g · cm
M_{sc}	2000 kg
ρ_{areal}	25 kg/m ²
a_{RES}	0.5 × 10 ⁻⁶ g
p_s	4.5 × 10 ⁻⁶ k N/m ²

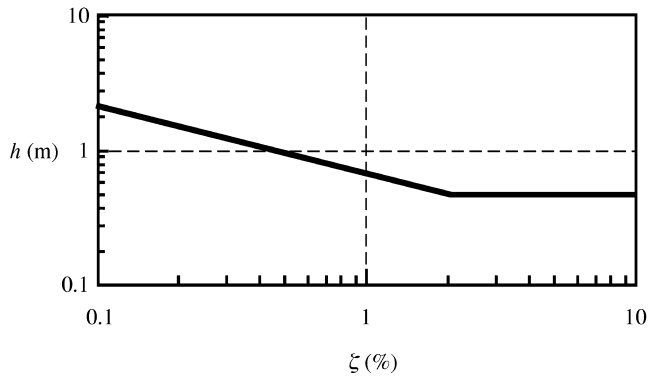


Fig. 11 Primary mirror truss depth requirement.

enhancing the damping above 2% by means of active-control will not reduce the mass of the structure.

The frequency requirements in Fig. 10 can be further related to the depth requirement for the primary mirror structure by using Eq. (22). For this purpose, the primary mirror was assumed to be a honeycomb ULE facesheet supported by a graphite epoxy truss. Only the truss is assumed to provide stiffness. To improve the accuracy of this analysis, Eq. (22) is generalized to consider all vibration modes of the reflector. Then, the mode with the greatest effect on the wave front is selected. To do this, Eq. (22) is written in more general form as

$$f_{ij} = \frac{\lambda_{ij}^2}{D} \cdot \frac{h}{D} \cdot \sqrt{\frac{\eta E}{\rho}} \quad (53)$$

where the eigenvalue λ_{ij} corresponds to the mirror vibration mode with the greatest effect on the wave front. For this example, the critical vibration mode has a radial wave number of 1.5, a circumferential wave number of 0.5, and an eigenvalue $\lambda_{ij} = 14.4$. Note that this is not the lowest mode of the structure, but rather the lowest mode that has the spatial variation most important to the wave front.

Figure 11 presents a plot of the primary-mirror-support-truss depth that is needed to meet the frequency requirement defined in Fig. 10. These results are derived from Eq. (53) and assume a structural mass fraction $\eta = 0.17$ and a material specific modulus $E/\rho = 1.36 \times 10^8 \text{ m}^2/\text{s}^2$. For a damping ratio of 1%, the depth needs to be approximately 0.7 m. Because of the control sensor resolution requirement, the minimum acceptable depth for the truss would be approximately 0.5 m. However, the required depth approaches 2 m when the damping level becomes very low.

This example illustrates a method for considering both vibration frequency and damping simultaneously in the conceptual design of a large-space-structure. A large space telescope was selected because of the very strict requirements that such an instrument places on the structure and active-control systems. In general, it is seen that increased damping, either from passive or active means, can reduce the vibration-frequency requirement, and hence the necessary structural depth. Optimal designs must consider this performance trade, as well as the issues of cost and complexity.

Summary

John M. Hedgepeth was one of an elite group of structural engineers who led NASA's revolutionary research on large space structures during the 1970s and 1980s. He had an incisive ability to distill, for unique and complex structural design problems, a concise set of primary requirements and to develop back-of-the-envelope analytical expressions that relate key design parameters to critical performance metrics. Several such back-of-the-envelope solutions, some by the authors and one by Dr. Hedgepeth, to fundamental problems in the design of large-space-structures have been presented. Although these derivations do not exist in the traditional literature on structural design, they are based on traditional concepts

from mechanics, dynamics, and stability theory. Similarly, the derivations involve relatively straightforward, although not necessarily obvious, mathematical formulations.

The analyses were focused on several issues that affect substantially the conceptual design of a large-space-structure. In particular, following Dr. Hedgepeth's approach, the analyses presented herein have identified the following fundamental conclusions relevant to large-space-structure design:

- 1) The use of trusses in the construction of large space structures largely derives from consideration of compression-strength efficiency and minimum-gauge construction issues.
- 2) All trusses made of the same material must have the same bulk modulus-to-density ratio; any two trusses with the same stiffnesses must also have the mass (neglecting joint and parasitic masses).
- 3) The vibration frequency of an areal truss tends to be proportional to its depth and the square root of its structural mass; an increase in depth allows a decrease in mass, and vice versa.
- 4) The deformation of a truss due to any inertial load is proportional to the sum of the inverse squares of the natural frequencies of the structure.
- 5) The mean square surface distortion of a truss due to member length errors is proportional to the sum of the inverse squares of the natural frequencies of the structure.
- 6) Increased damping, either from passive or active means, can reduce the vibration-frequency requirement, and hence the necessary structural depth for a given application.

Acknowledgments

The example application of a large space telescope was taken from work sponsored by Boeing-SVS under contract number 03176. This work was performed in support of Jet Propulsion Laboratory, California Institute of Technology Contract 1242231, which was awarded as part of NASA NRA 01-OSS-04 "Extra-Solar Planets Advanced Mission Concepts."

References

- [1] Hedgepeth, J. M., "Critical Requirements for the Design of Large Space Structures," NASA CR-3484, 1981.
- [2] Schuerch, H. U., and Hedgepeth, J. M., "Large Low-Frequency Orbiting Radio Telescope," NASA CR-1202, 1968.
- [3] MacNeal, R. H., Schuerch, H. U., and Hedgepeth, J. M., "Heliogyro Solar Sailer Summary Report," NASA CR-1329, June 1969.
- [4] Hedgepeth, J. M., "Dynamics of a Large Spin-Stiffened Deployable Paraboloidal Antenna," *Journal of Spacecraft and Rockets*, Vol. 7, No. 9, Sept. 1970, pp. 1043-1048.
- [5] Hedgepeth, J. M., Crawford, R. F., and Preiswerk, P. R., "Spoked Wheels to Deploy Large Surfaces in Space: Weight Estimates for Solar Arrays," NASA CR-2347, Jan. 1975.
- [6] Hedgepeth, J. M., and Crawford, R. F., "Effects of Initial Waviness on the Strength and Design of Built-Up Structures," *AIAA Journal*, Vol. 13, No. 3, March 1975, pp. 672-675.
- [7] Hedgepeth, J. M., "Survey of Future Requirements for Large Space Structures," NASA CR-2621, Jan. 1976.
- [8] Hedgepeth, J. M., Coyner, J. V., and Riead, H. D., "Long-Boom Concepts," NASA CR-145169, Sept. 1976.
- [9] Hedgepeth, J. M., "Ultralightweight Structures for Space Power," *Radiation Energy Conversion in Space: Technical Papers Prepared for the Third NASA Conference on Radiation Energy Conversion*, AIAA, New York, 1978.
- [10] Hedgepeth, J. M., Mikulas, M. M., and MacNeal, R. H., "Practical Design of Low-Cost Large Space Structures," *AIAA Journal*, Vol. 16, Oct. 1978, pp. 30-34.
- [11] Hedgepeth, J. M., and Miller, R. K., "The Buckling of Lattice Columns with Stochastic Imperfections," *International Journal of Solids and Structures*, Vol. 15, No. 1, 1979.
- [12] Hedgepeth, J. M., Knapp, K. K., and Finley, L. A., "Structural Design of Free-Flying Solar-Reflecting Satellites," *Society of Allied Weight Engineers Journal*, Vol. 39, No. 2, 1979, pp. 7-24.
- [13] Hedgepeth, J. M., and Mikulas, M. M., "Expandable Modules for Large Space Structures," AIAA Paper 79-0294, May 1979.
- [14] Hedgepeth, J. M., "Influence of Interorbit Acceleration on the Design of Large Space Antennas," *LSST/Low Thrust Propulsion Technology Information Exchange Meeting*, NASA CP-2144, May 1980.

- [15] Hedgepeth, J. M., "Efficient Structures for Geosynchronous-Spacecraft Solar Arrays," *Space Photovoltaic Research and Technology Conference*, NASA CP-2169, Oct. 1980.
- [16] Hedgepeth, J. M., Miller, R. K., and Knapp, K. K., "Conceptual Design Studies for Large Free-Flying Solar-Reflector Spacecraft," NASA CR-2438, June 1981.
- [17] Hedgepeth, J. M., MacNeal, R. H., Knapp, K. K., and MacGillivray, C. S., "Considerations in the Design of Large Space Structures," NASA CR-165744, Aug. 1981.
- [18] Hedgepeth, J. M., "Influence of Fabrication Tolerances on the Surface Accuracy of Large Antenna Structures," *AIAA Journal*, Vol. 20, No. 5, May 1982, pp. 680–686.
- [19] Hedgepeth, J. M., "Accuracy Potentials for Large Space Antenna Reflectors with Passive Structure," *Journal of Spacecraft and Rockets*, Vol. 19, No. 3, May–June 1982, pp. 211–217.
- [20] Hedgepeth, J. M., and Adams, L. R., "Design Concepts for Large Reflector Antenna Structures," NASA CR-3663, Jan. 1983.
- [21] Hedgepeth, J. M., Mobley, T. B., and Taylor, T. C., "Support Structures for Large Infrared Telescopes," NASA CR-3800, July 1984.
- [22] Hedgepeth, J. M., and von Roos, A., "Design, Model Fabrication, and Analysis of a Four Longeron, Synchronously Deployable, Double-Fold Beam Concept," Astro Aerospace Corporation AAC TN-1139, March 1985.
- [23] Hedgepeth, J. M., "New Concepts for Precision Reflector Support Structures," *36th International Astronautical Federation Congress*, International Astronautical Federation Paper 85-208, 1985.
- [24] Hedgepeth, J. M., "Evaluation of Pactruss Design Characteristics Critical to Space Station Primary Structure," NASA CR-178171, Feb. 1987.
- [25] Hedgepeth, J. M., and Miller, R. K., "Structural Concepts for Large Solar Concentrators," *Acta Astronautica*, Vol. 17, No. 1, Jan. 1988, pp. 79–89.
- [26] Hedgepeth, J. M., "Structures for Remotely Deployable Precision Antennas," Astro Aerospace Corporation, Rept. AAC TN-1154, Jan. 1989.
- [27] Hedgepeth, J. M., and Miller, R. K., "Investigation of Structural Behavior of Candidate Space Station Structure," NASA CR-181746, June 1989.
- [28] Hedgepeth, J. M., "Pactruss Support Structure for Precision Segmented Reflectors," NASA CR-181747, June 1989.
- [29] Hedgepeth, J. M., and Thomson, M., "Space-Based Radar Deployable Antenna Structure Survey: Final Report," Astro Aerospace Corporation, Rept. AAC-TN-1158, Nov. 1989.
- [30] Mikulas, M. M., Collins, T. J., and Hedgepeth, J. M., "Preliminary Design Considerations for 10 to 40 Meter-Diameter Precision Truss Reflectors," *Journal of Spacecraft and Rockets*, Vol. 28, No. 4, July–Aug. 1991, pp. 439–447.
- [31] Hedgepeth, J. M., Thomson, M., and Chae, D., "Design of Large Lightweight Precise Mesh Reflector Structures," Astro Aerospace Corporation, Rept. AAC TN-1164, Nov. 1991.
- [32] Hedgepeth, J. M., and Lawrence, C., "Design of Structures for Nuclear Electric Propulsion Vehicles," *34th AIAA/ASME/ASCE/AHS/ASC SDM Conference*, AIAA Paper 93-1393, 1993.
- [33] Hedgepeth, J. M., "Structures for Solar Electric Propulsion Vehicles," Digisim Rept. DCR-7, March 1993.
- [34] Hedgepeth, J. M., "Interaction Between an Inflated Lenticular Reflector and its Rim Support," *36th AIAA/ASME/ASCE/AHS/ASC SDM Conference*, AIAA Paper 95-1510, 1995.
- [35] Roark, R. J., and Young, W. C., *Formulas for Stress and Strain*, 5th ed., McGraw-Hill, New York, 1982.
- [36] Blevins, R. D., *Formulas for Natural Frequency and Mode Shape*, Krieger, Malabar, FL, 1995.
- [37] Brush, D. O., and Almroth, B. O., *Buckling of Bars, Plates, and Shells*, McGraw-Hill, New York, 1975.
- [38] Mikulas, M. M., "Structural Efficiency of Long and Lightly Loaded Truss and Isogrid Columns for Space Applications," NASA TM-78687, July 1978.
- [39] Lake, M. S., "On the Analysis and Design of Uniform Truss Structures," Ph.D. Dissertation, North Carolina State Univ., Raleigh, NC, May 1992, pp. 53–62.
- [40] Neyfeh, A. H., and Hefzy, M. S., "Continuum Modeling of Three-Dimensional Truss-Like Space Structures," *AIAA Journal*, Vol. 16, No. 8, Aug. 1978, pp. 779–787.
- [41] Novozhilov, V. V., *Theory of Elasticity*, Sudpromgiz, Leningrad, 1958 (in Russian); translation by Program for Scientific Translations, Jerusalem, 1961, pp. 132–135.
- [42] Lake, M. S., Peterson, L. D., and Levine, M. B., "A Rationale for Defining Structural Requirements for Large Space Telescopes," *Journal of Spacecraft and Rockets*, Vol. 39, No. 5, Sept.–Oct. 2002, pp. 674–681.
- [43] Wu, K. C., and Lake, M. S., "Natural Frequency of Uniform and Optimized Tetrahedral Truss Platforms," NASA TP-3461, Nov. 1994.
- [44] Melody, J. W., "Discrete-Frequency and Broadband Reaction Wheel Disturbance Models," NASA Jet Propulsion Lab., California Inst. of Technology Interoffice Memorandum 3411-95-200csi, 1 June 1995.
- [45] Griffin, M. D., and French, J. R., *Space Vehicle Design*, 1st ed., AIAA, Washington, DC, 1991, pp. 128–130.

V. Zoby
Associate Editor